

Research Article | Volume 13, Issue 3 | Pages 536-546 | e-ISSN: 2347-470X

Mitigating in Band Overshoot in Digital High-Pass Filters: Design and Analysis of Bessel and Gaussian Filters for Maximally Flat Step Response

Hussein Shakor Mogheer¹, Alrubei Mohammed A.T.², Yassir AL-Karawi³

¹Research Lecture, Department of Communication Engineering, College of Engineering, University of Diyala, Baqubah 32001, Iraq ²Assistant Professor, Department of Electronics and Communication Techniques, Al-Najaf Technical Institute, Al-Furat Al-Awsat Technical University, Najaf 54001, Iraq

³Assistant Professor, Department of Communication Engineering, College of Engineering, University of Diyala, Baqubah 32001, Iraq

ABSTRACT- Digital high-pass filters play an important role in transcending the low-frequency noise to maintain the signal integrity in several modern applications of communication systems. The most important distinction between them is the attempt to obtain a flat step response and a minimum of distortion in the amplitude-frequency response (AFR). The trade-off between flat step response and the minimum amplitude-frequency response distortion in IIR high-pass filters generated by bilinear transformations of Bessel and Gaussian low-pass prototypes is explored in this paper The proposed design uses a parallel structure where the amplitude frequency response of the low-pass filter is subtracted from the direct pass AFR to eliminate step response overshoot without sacrificing time-domain flatness. Filter performance is validated and overshoot behavior quantified using numerical evaluations performed in the Mathcad environment. Comparison of various filter orders in parallel and stage-by-stage connections shows that Gaussian-based HPFs have minimal negative step overshoot (as low as -0.002%) compared to Besselbased filters (e.g., -0.37% for 8^{th} order). However, AFR overshoot increases with order (72% for Gaussian, 78% for Bessel). The parallel scheme reduces the AFR overshoot by up to 30% over the conventional schemes without degradation in transient response and results in robust low-distortion filters in real-time detection applications.

Keywords: AFR overshoot, Bessel and Gaussian filters, Bilinear transformation, Digital high-pass filters (HPFs), Group delay, Step response, In-band frequency overshoot mitigation, Maximally flat step response.

ARTICLE INFORMATION

Author(s): Hussein Shakor Mogheer, Alrubei Mohammed A.T., Yassir AL-Karawi;

Received: 11/05/2025; Accepted: 28/08/2025; Published: 30/09/2025;

E- ISSN: 2347-470X; Paper Id: IJEER 1105-06; Citation: 10.37391/ijeer.130318

Citation: 10.37391/ijeer.1 Webpage-link:

https://ijeer.forexjournal.co.in/archive/volume-13/ijeer-130318.html

Publisher's Note: FOREX Publication stays neutral with regard to jurisdictional claims in Published maps and institutional affiliations.

1. INTRODUCTION

1.1.Background and Motivation

Website: www.ijeer.forexjournal.co.in

In high-fidelity digital signal processing (DSP) systems, especially biomedical (e.g., electrocardiography: electrocardiography (ECG) and electroencephalography (EEG)), the interference of signal distortion reduces the diagnostic accuracy of the equipment [1],[2]. Large negative overshoot of step response in digital high-pass filters (HPFs) causes false detections or quenching of small signal characteristics as a primary source of such distortion [3],[4]. Flatness of the step response thus must be ensured in all systems

where time-domain characteristics are critical to performance and reliability [2],[5]. A simple use of HPFs is to eliminate signal of low frequencies (offset, flicker noise etc.), which hide useful high-frequency information after being converted to digital signals by an analog-to-digital converter [6],[7], [35]. However, the synthesis of HPFs, especially within high-speed settings, has to go around challenges inherent in attaining ideal trade-offs amid temporal and spectral performance behavior [8],[9].

Most common digital advanced high-pass filter (HPF) designs (Butterworth filters, Chebyshev Type I and Type II, and Elliptic filters) can be derived by analogy-to-analog transformation of analog low-pass prototypes [7],[10]. Although their designs provide sharp cutoff characteristics and acceptable amplitude-frequency response (AFR) selectivity, their performance is generally poor with regard to step-response characteristics, i.e., ripples and negative overshoot, due mostly to the higher-order versions [11],[12]. These skews are especially undesirable in high-resolution time-domain applications where they may cause a false exclusion or cause clinically important portions of the signal to merge together [3],[4].

The Bessel and Gaussian filters, in contrast, have smooth and monotonic step responses that are inherently smooth, have a

^{*}Correspondence: Hussein Shakor Mogheer, Email: hussein alkarawi eng@uodiyala.edu.iq



Research Article | Volume 13, Issue 3 | Pages 536-546 | e-ISSN: 2347-470X

nearly constant phase, and have a flat group delay [2],[13]. These characteristics render them special applications in terms of the waveform preservation and time distortion deterrence in mission-sensitive services like in biomedical machinery and precision indicator systems [14],[15]. Nonetheless, even its digital usages, more so in higher demand, are vulnerable to AVR emissions at close-to-cut-off frequencies [16], [17]. It is this inherent time-frequency trade-off that drives the quest to seek better design methodologies that will be able to capture the time-domain advantages of Bessel and Gaussian prototypes but provide a solution to their limitations in the frequency domain [18],[19].

This has been addressed in the recent studies by attempting to overcome this challenge using adaptive filter structures, parallel designs, multi-stage designs, and hybrid filtering methods [18],[20]. Nevertheless, it is hard to achieve a good trade-off between step response flatness and spectral selectivity in real systems, as much as has been tried to shape the step response [17],[21].

1.2.Literature Review and Research Gaps

The High-pass filters (HPFs) are crucial in DSP when it comes to the removal of the low frequency that interferes with and distorts the clarity and reliability of the extracted signals, a phenomenon that is usually referred to as DC offsets and flicker noise [6],[7]. One of the most important design objectives of IIR HPFs is the ability to obtain a flat step response so as to maintain signal fidelity, where excess overshoot in biomedical applications can result in unwanted triggering or inaccurate interpretations [4],[5]. This is particularly important when seeking negative or weak signals based on positive impulse patterns as it is the case with real time monitoring systems [3],[14].

Analog prototypes are typically chosen to be converted to digital form, such as the Bessel or Gaussian filters since they have smooth step responses and desirable time domain properties by nature [2],[13]. Bilinear transformation technique is widely used to transfer these analog filters to the respective digital filters [3], [22]. Gaussian filters have facilitated excellent monotonic step response; Bessel filters present almost linear phase and a straight-line group delay, which are of vital importance when ensuring signal integrity in the time domain [13],[22]. When the filters are used in a digital implementation, particularly once of higher order, either will potentially include amplitude-frequency response (AFR) overshoot at the cutoff frequency, thus creating a traditional trade-off between spectral and temporal characteristics [16],[17]. In modern designs, cascaded structures equipping parallel or stage-by-stage Bessel and Gaussian or Bessel and of odd orders low-pass filter blocks with phase inversion are being adopted to optimize the measure of flatness of the step response and spectral overshoot control, trading off performance measures such as mean squared error (MSE) rise and settling times and percent overshoot [15],[18]. These filter designs are computationally lightweight and wellsuited to real-time embedded systems and thus find application in FPGA and ASIC implementations, such as those used in

Website: www.ijeer.forexjournal.co.in

sensitive signal detection tasks where low false detection rates and robust time-frequency response is vital [9],[21], [32],[36]. The solution to the problems has been met in different methods of designing filters, which include rearranging the structure, enhancing the settings, and employing various stages of the filtering procedure [18],[19]. The use of more sophisticated approaches, such as Particle Swarm Optimization (PSO) or hybrid PSO with some other approaches, has been recently employed to improve the nature of the filters to come up with better results in the recent past [4],[23], [38]. The practices assist in regulating the place where the filters operate and how steady they are, particularly in circumstances where restrictions occur on defining the settings precisely and where the filters may fail to perform as anticipated [19], [24]. The positive part about IIR filters is that they have a simple design and fewer components compared to the FIR filters. But the effectiveness of their working may depend on the settings applied both initially and after their operating period. To take an example, it may overshoot, or continue to ring, unless exceedingly careful settings are used; this is relevant in medical uses, such as heart and brain monitoring [14],[25]. The FIR filters, however, are only desired because they operate without ripples and overshoot, though they require more components, thereby causing them to be slower and more powerful-consuming [21],[26].

These issues will be solved by employing methods such as Particle Swarm Optimization (PSO), and a combination of Taguchi and Genetic Algorithm (HTGA), to make robust IIR-filters [23],[27], [37]. Bilinear transformation contributes the distortion in the frequency domain that should be controlled to ensure the required specifications are fitted [28],[29]. The aim of this is to translate the frequency axis of the digital part into the analog prototype via some scaling constants. Nevertheless, it is still challenging to satisfy simultaneously both time-domain and frequency-domain condition [17],[21].

Several publications are available using Gaussian and Bessel filters in processing ECG signals and also in phasor measurement of power systems [14],[15]. They need to be applied in cases such as where there is a need to detect the signals reliably, suppress drifts, and preserve frequencies [25], [30]. The domains, however, tend to be traded-offs during the design process [17],[26]. FIR filters do well at filtering noise off of ECG signals but require a lot of computer power. IIR filters are faster and there is the possibility of overshooting due to excessively high cut-off [3],[16]. So, there occurs an increasing demand as well that digital filter features can optimize these inconsistent performance metrics [21], [24].

However, regardless of these developments, there are a number of important gaps in the existing literature:

- Single-sided optimization emphasis: Much of the previous work resorts to optimization in the time-domain (such as step response flatness) or frequency-domain (such as AFR control) with relatively little work being done to achieve optimization in both domains in a combined manner.
- Insufficient structural analysis between filter orders: Not many works have been presented on the impacts of filter orders on critical measures of performance, namely step



Research Article | Volume 13, Issue 3 | Pages 536-546 | e-ISSN: 2347-470X

response and AFR overshoot, where the reason is architectural variation.

- There is little use of parallel digital structures. The current designs are typically: based on single-stages implementation or coefficient tuning. A combination of parallel digital structures based on a bilinear transformation of analog prototypes, like Gaussian or Bessel filters, is not integrated into other previous works.
- Lack of direct comparative comparisons: As much as there are studies that compare the application of both Bessel and Gaussian filters, there are limited articles that specifically compare the application in sequential order, particularly in the aspect of the AFR performance or the stability of the time-domain under a single experimental scenario. The structural trade-offs that are inherent are not discussed enough.

1.3. Contributions of the Paper

This paper shows a new implementation of the digital high-pass filter (HPF) using a parallel architecture of high-order Gaussian, and Bessel low-pass filters to develop the filter with a maximally flat step response and significantly a smaller overshoot in the amplitude-frequency response (AFR). The resulting benefit of this proposed configuration consisting of a combination of direct signal path along with a phase-inverted low-pass branch is to utilize the naturally smooth time-domain performance of the Gaussian and Bessel filters to efficiently counter the otherwise linear-phase error-producing frequencydomain overshoot inherent to uncompensated traditional designs and tends to increase with filter order. A methodical comparison of the effect in various filter order manifests an AFR overshoot reduction that is uniformly 20-30% in comparison to the equivalent order multi-stage implementation, and with no time-domain deterioration. The contributions provide an effective and bandwidth-scalable approach to timely and computationally demanding applications like biomedical instrumentation [1], real-time control [31], and audio signal processing that requires simultaneous compromise of time- and frequency-domain properties [32], [33]. A large comparison table is availed in Table 1 of classical and proposed digital highpass filter designs outlining the superiority of the proposed methodology in time-domain flatness and frequency-domain overshoot performance. The background motivation of the proposed design approach which follows can be found in this comparative summary (Table 1 and Table 2).

Table 1. Comparative summary of classical and proposed high-pass filter designs

Filter Type	Step Response Flatness	AFR Overshoot
Butterworth	Moderate	Low
Chebyshev I	Poor (ripples)	High
Chebyshev II	Poor (ripples)	Moderate
Elliptic	Poor (ripples)	Very high
Bessel	Excellent	Higher
Gaussian	Excellent	Higher
Proposed Work	Excellent	Controlled

Website: www.ijeer.forexjournal.co.in

Table 2. Comparative summary of classical and proposed high-pass filter designs

Notes	Design Technique / Method	Key References
Maximally flat AFR, but slow roll-off	Classical analog prototype + Bilinear	[6],[27]
Passband ripple	Classical pole placement	[5],[18]
Stopband ripple	Classical zero placement	[5],[6]
Sharpest cutoff, ripple in both bands	Minimax optimization	[16],[21]
Flat group delay	Classical analog + Bilinear	[17],[22]
Monotonic and smooth response	Classical analog + Bilinear	[5],[6]
Time/frequency Trade-off balance	Parallel block upon bilinear technique of Bessel/Gaussian analogs+ qualitative structural analysis (AFR, MSE, rise/settling)	-

The remainder of this paper is structured as follows: Section 2 contains a literature review of the vital concepts and problems in the design of the digital high-pass filters with Bessel and Gaussian prototypes. In section 3 a parallel block structure is given to clear the overshoot of step response. Section 4 has mentioned the structural description of mathematical formulation and the performance metrics. A discussion of how filters behave in the presence of group delay within the direct signal path is in section 5. Lastly, Section 6 gives a conclusion to the paper and outlines possible directions of future investigation.

2. PROBLEM FORMULATION

Eliminating the low-frequency components and associated noise is crucial in many signal processing systems, particularly biomedical ones, so that the signal can be clearly perceived and its readings can be accurately interpreted after it has been converted to digital form [6], [34]. Moreover, designing a digital high-pass filter (HPF) which can do so without altering the shapes of transient signals has proved to be a highly technical task [10], [20].

Whether high-pass filtering (HPF) or other data-processing methods, like regression analysis, should be used to analyze electroencephalographic (EEG) signals has been long debatable scientifically. Experimental results depict that HPF has the better performance whenever the step response of the filter has either a flat or nearly flat response curve [3], [15], [18]. The step response of the 1st order Bessel, Gaussian, types I and II Chebyshev, and Butterworth high-pass filters alongside its elliptic counterpart maintains a flat characteristic, but it is frequently not employed because spectra of the upper range of the flicker noises (low-frequency noises, the spectral density of which is inversely proportional to its frequency) and a lower limit of the valuable signal can be very near one another in the frequency axis.



Research Article | Volume 13, Issue 3 | Pages 536-546 | e-ISSN: 2347-470X

A higher-order filter is required to filtrate (to suppress) flicker noises in this case [34],[35]. However, the step response of the HPF beginning from the 2nd order and higher ones has ripples and a negative overshoot that is minimal for Gaussian filters. Studies examine digital high-pass filters that apply a flat step response, which are more optimized for flatness. Other filter properties (including AFR and PFR) are not used up to the maximum operating limits. The research team proposes the following digital IIR filters of the 1st, 2nd, 4th and 8th orders to be implemented.

3. TIME-DOMAIN HIGH-PASS FILTER APPROACHES ANALYSIS

3.1. Analyzing Step Responses Varying High-Pass Filter Types

Figure 1(a-f) compares the step response comparison of five high-pass filters which includes Bessel with Gaussian, both Type I and Type II Chebyshev, Butterworth and an elliptic filter with the 5th order highlights significant differences in timedomain behavior. All designs share a relative cutoff frequency of 0.00025 that appears at this point and in subsequent sections. The conversion to digital filters occurs through bilinear transformation of their analog prototypes. While the amplitudefrequency responses exhibit linear dependence on the ordinate and maintain nearly linear phase and group-delay characteristics, clear differences emerge in the time domain. Gaussian HPF generates a step response with higher flatness levels than alternative HPF versions as illustrated in Figure 1(a). The step response output of a Bessel filter demonstrates higher variations in amplitude compared to its fellow filters when measuring response to input signals.

3.2. Comparison of Digital Gaussian and Bessel HPFs Step Responses *via* Order-Dependent

Analyzing figure 2(a-d) allows one to observe the step-response profile of Gaussian HPFs of 1st, 2nd, 4th and 8th orders as well as their respective low-pass versions. Order increment leads to greater low-frequency attenuation at the cost of small-amplitude oscillations in the step response even in Gaussian designs, which are nonetheless very much smaller than in other filter families, leaving them suitable to ECG/EEG processing. But the amount of AFR overshoot increases with order, as is natural due to the time-frequency trade-off inherent in high-order designs. The most common representation of such a trade-off, necessitated by the requirements of steep roll-off and a high stopband attenuation, is the consequent ringing and overshoot in the time domain.

The success of steep roll-off followed by stopband attenuation in the frequency domain will induce time-domain errors that are pronounced by ringing and overshoot. The engineers minimize this effect in two ways involving the choice of filters of a certain type (Bessel in step-critical applications) and the use of post-processing (equalization, all-pass phase correction).

The Steady-state passband performance is within requirements, but the outside and the selected band-specification requirement illustrates how transition frequency signals/stopband have the

ability to influence the transients but do not impact the typical passband requirements [9].

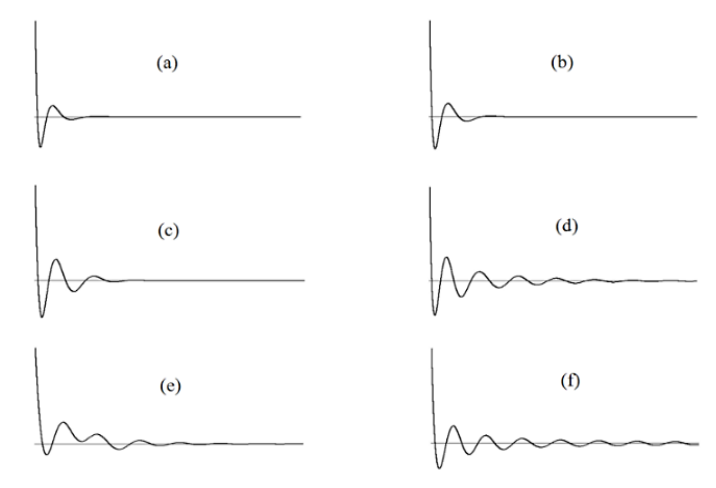


Figure 1. SRs of the fifth-order high-pass filters: (a) The Gaussian filter; (b) The Bessel filter; (c) The Butterwort filter; (d) Chebyshev type I filter; (e) Chebyshev type II filter; (f) The elliptic filter. All axes and abscissa readings use linear scales for this appearance

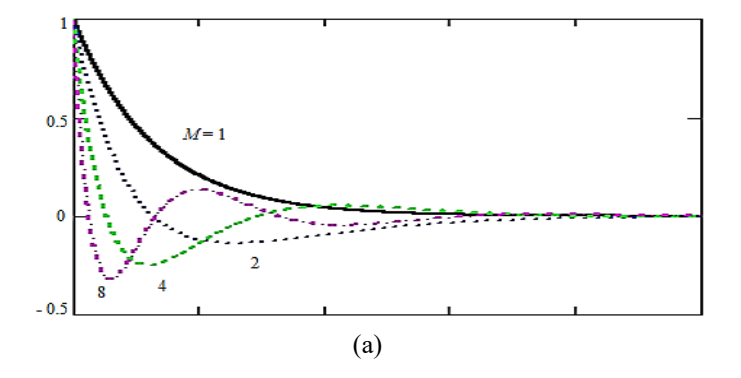


Figure 2. SRs of Gaussian HPFs: (a) First order filter; (b) Second order filter; (c) Fourth order filter; (d) Eighth order filter. All axes and abscissa readings use linear scales for this appearance

3.3. Amplitude-Frequency Responses and The SRs Performance of HPFs with 1st Order Sequentially Connected

Connecting multiple first-order high-pass filters in stages creates step response ripples which appear in the system output The amplitude-frequency and step responses of the 1^{st} order with M high-pass filter joining sequentially (stage-by-stage) are represented in *fig. 3 (a)* and *(b)* with M=1; M=2; M=4 and M=8, where the same is calculated using the bilinear transformation method.

Creating flat step responses in digital HPF block diagrams stands as an important research priority that requires design work although the other features such as AFR and PFR could remain sub-optimal [9].



Research Article | Volume 13, Issue 3 | Pages 536-546 | e-ISSN: 2347-470X

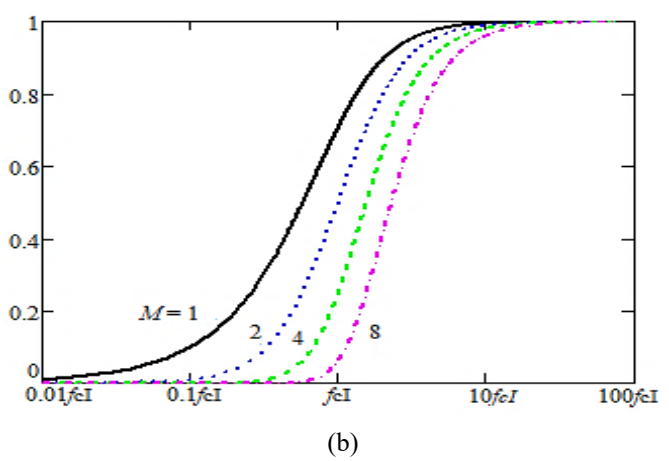


Figure 3. (a) SRs of M at various values equal to 1, 2, 4, 8 show equivalent results of high-pass filters with the 1st order LPFs and stage-by-stage connection, (b) AFRs of these filters $(f_c$ is of the 1st order LPF)

4. PROPOSED METHODOLOGY FOR HPFs DESIGN AND ANALYSIS

4.1. Analysis of Parallel System Configurations with Transfer Function Subtraction

The proposed design optimizes step response flatness in highpass filters through parallel implementation of direct signal paths combined with low-pass filter branches and phase inverted connection as depicted in *figure 4(a)* (where the AFR of direct-pass to produce the filter output is subtracted by the LPF AFR). The mathematical relations are given by *eq. (1)* to (3), which establish that a flat step response in the LPF ensures an equally flat response in the derived HPF. The proposed design structure enhances transient response functionality that can be expressed by *eq. (1)*

$$H_{HPF}(z) = 1 - H_{LPF}(z)$$
 (1)

Where: 1 is a transfer function of the direct pass; $H_{LPF}(z)$: is the mathematical structure of LPF transfer function.

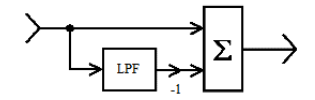
Converting a transfer function into a frequency response is achieved by means of the following substitution: $z \to e^{j\omega T}$, Where $\omega = 2\pi f$ is a angular frequency; f: is a regular frequency; T: is a period (a step) of sampling. As a result of substituting, the frequency transfer function is clarified in eq. (2)

$$H_{HPF}(e^{j\omega T}) = 1 - H_{LPF}(e^{j\omega T}) \tag{2}$$

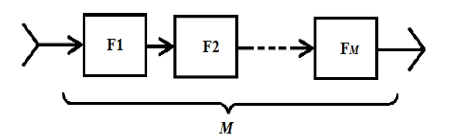
Figure 4(a) shows that: The feeding of HPF input by a unit step 1(n) results in an output determined by subtracting $a_{LPF}(n)$ of the LPF step response. Hence, the response to a step input for the HPF will be defined by eq. (3).

$$a_{HPF}(n) = 1 - a_{LPF}(n) \tag{3}$$

By consequence, a monotone step response of an LPF also has a monotone response to an HPF. The linear programming filters which have flat step responses are started with the analysis [9].



(a) A parallel HPF based on subtracting the LPF AFR from the direct pass AFR



(b) Stage-by-stage of the M filters

Figure 4. The proposed HPF block diagram

4.2.Performance Assessment Metrics

To determine how the simulated digital high-pass filters proceed dynamically, some performance metrics are defined. The step response y(n) acquired from the discrete-time simulation is checked as compared with the ideal step response $y_{ideal}(n)$, which is the theoretical benchmark. Where the type of observation window is restricted to N samples.

The transient response fidelity is measured by the Mean Squared Error which is calculated as the average of the squared difference between y(n) and $y_{ideal}(n)$.). In addition to the previous, one also obtains time-domain parameters: the rise time (it is the time required to attain between 10% and 90% of the final steady-state value y_{final})) and the settling time (the time it takes when the response is within a tolerance band ($\pm 2\%$ or $\pm 5\%$ of y_{final})). The metrics give a systematic approach to the evaluation of filter performances and allow consistent comparisons across Gaussian and Bessel prototypes of varying orders. These definitions are formally expressed by the mathematical relations presented in equations (4) to (6).

Mean Squared Error (MSE):

$$MSE = \frac{1}{N} \sum_{n=1}^{N} [y(n) - y_{ideal}(n)]^{2},$$
 (4)

Where: y(n) is the computed step response at sample n, $y_{ideal}(n)$ is the corresponding value of the ideal step at that sample, and N is the total number of samples.

Rise Time (t_r):

Rise Time =
$$t_{90\%} - t_{10\%}$$
, (5)

Where: $t_{10\%}$ and $t_{90\%}$ are the times at which the step response first exceeds 10% and 90% of its final steady-state value, respectively.

Settling Time (t_s) : is the time prescribed for the response to persist in accordance with a particular tolerance band (Ordinarily $\pm 2\%$ or $\pm 5\%$ of the final value) following a step input and not deviate outside it afterwards:

Settling Time =
$$t_{when} |y(t) - y_{final}| < tolerance $\forall t > ts$, (6)$$

Research Article | Volume 13, Issue 3 | Pages 536-546 | e-ISSN: 2347-470X

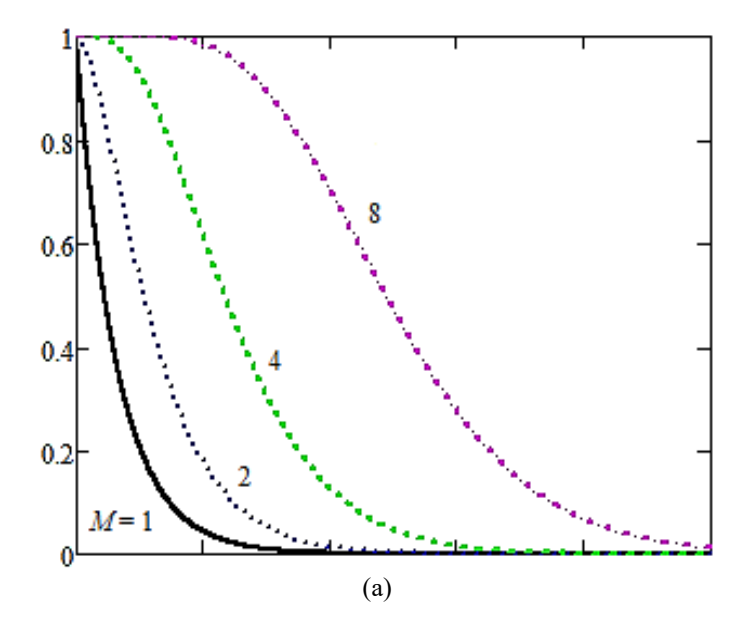
Where: y(t): is the step response at time t, and y_{final} : is the steady-state value.

These parameters are essential to systematically present filter performance in simulation so they can be compared across different filter designs, orders, and types. By utilizing these measures in a controlled simulation environment, researchers will be able to objectively measure the trade-offs between transient response and frequency response, and the eventual optimization of digital HPFs to meet applications where signal integrity and distortion are critical design considerations.

4.3. HPFs Based on a Cascade First-Order LPFs Connections in Parallel Block Diagram

Steeper roll-off can be achieved by making use of higher-order Gaussian or Bessel LPF (orders 1, 2, 4, 8) in the parallel configuration, without drawback to step-response flatness. But, the AFR overshoot gets bigger with order and it is important that the cutoff frequencies are chosen carefully so as not to compromise both the noise suppression and the transient integrity. The filter obtained is applied in parallel block diagram as described in *figure 4(a)*. Moreover, the *figure 4(b)* illustrates the cascaded-joint of the filtration units along the system. Moreover, the *figure 4(b)* exemplifies cascade nature of the filtration unit units across the system.

Response curves derived from block diagrams which featured M-LPFs of the $1^{\rm st}$ order (Gaussian, Bessel, Butterworth, Chebyshev filters of type II or elliptic one) arranged in parallel of stage-by-stage connections (M equals values to 1, 2, 4 and 8) present in $figure\ 5(a)$ are accompanied by their amplitude-frequency response shown in $figure\ 5(b)$. As illustrated in $figure\ 5(a)$, the HPFs step transients are flat; the cutoff frequency decreases with increasing M. The cascading connection of identical $1^{\rm st}$ order LPFs results in decreasing cutoff frequency due to the amplitude-frequency responses multiplying each other. Notice that the resulting HPF will be of the $M^{\rm th}$ order.



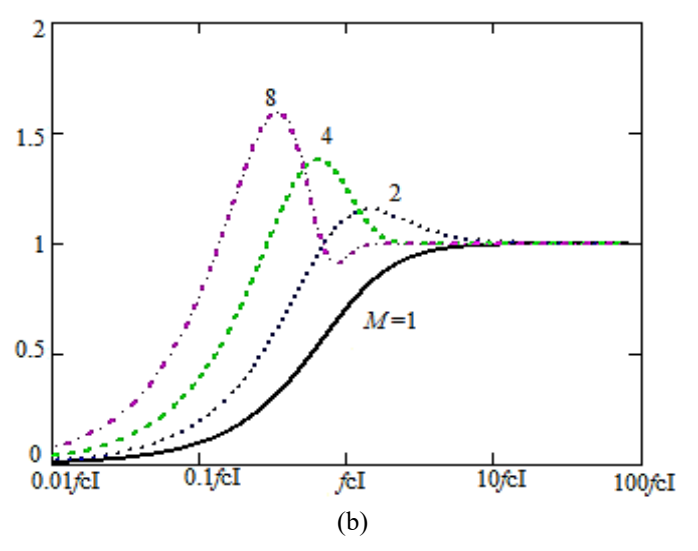


Figure 5. (a) SRs of high-pass filters formed using the parallel block layout of M low-pass filters 1st-order with stage-by-stage combination (M is equal to 1, 2, 4, 8). b) AFRs of these filters (f_c is of the 1st order LPF)

The stage-by-stage connection has a several the 1st order LPFs which is practically unlimited in the 1st stage. It allows the obtaining of a given slope of the AFR in the transition band. The step response together with phase-frequency characteristics and AFR parameters matches identically for 1st order LPFs (only the first order filter) across Butterworth, Chebyshev of type II, Gaussian, Bessel HPFs and elliptic filters. Analogously, a 1st order (1st only) HPFs have the same AFR, a phase and a step response for the used filters types.

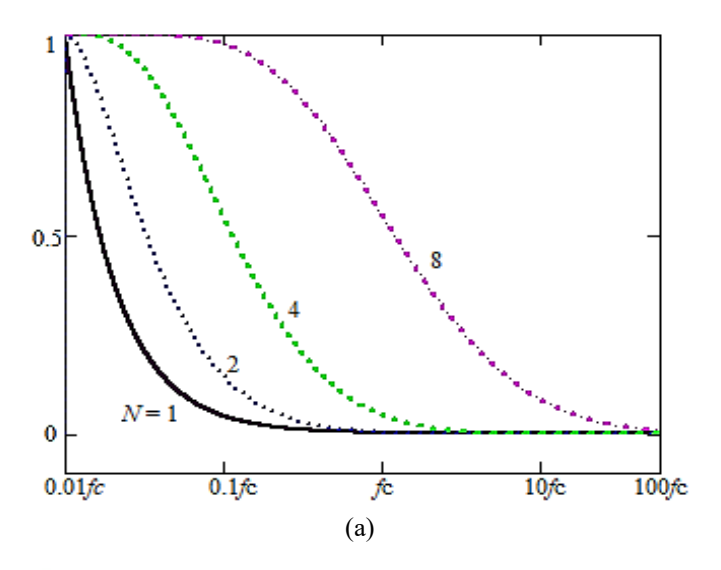
If the overshoot and ripples are present on the AFR of HPFs (Figure 5(b)), the parallel block schematic displays this as a disadvantage with M > 1 low-pass filers of 1st order and of the stage-by-stage connection. For M equal to 2, 4, 8, the values of a positive overshoot are of 15%, 38% and 59% respectively. A reason of the overshoot is a difference of the group delays in the arms of the parallel block diagram shown in figure 4(a) that does not lead to the direct (in-phase) subtraction of the LPF AFR from the direct pass AFR. The connection of a delay block into the direct pass results in the step response flatness loss, but in some cases, it reduces the amplitude-frequency response overshoots. The overshoot influence on the useful signal spectrum can be significantly reduced if one chooses, for example, $f_l/f_c = 10$, where f_l is a bottom frequency of the signal spectrum; f_c is the regular cutoff frequency of the 1st LPF. Nevertheless, with the overshoot and decrease of f_c present filtration of the flicker noises gets worse.

4.3. Applying LPFs of the higher order than the 1st order in the parallel block diagram

Gaussian and Bessel LPFs differ from the others in the better flatness of their step responses. The step response of the LPF of the 2nd order and higher one has ripples and the overshoot which are minimal for the Gaussian filter. Step responses and AFRs of the HPFs based on the parallel block diagram and realized with

Research Article | Volume 13, Issue 3 | Pages 536-546 | e-ISSN: 2347-470X

using the Gaussian LPF of the 1st, 2nd, 4th, and 8th orders are shown in *figure 6*. Here N is the LPF order that is equal to 1, 2, 4, 8. As can be seen from *figure 6(b)*, with increasing N, the cutoff frequency at the level of 0.707 decreases. The reason is that the cutoff frequency of Gaussian (and Bessel) filters is not specified to the level of 0.707.



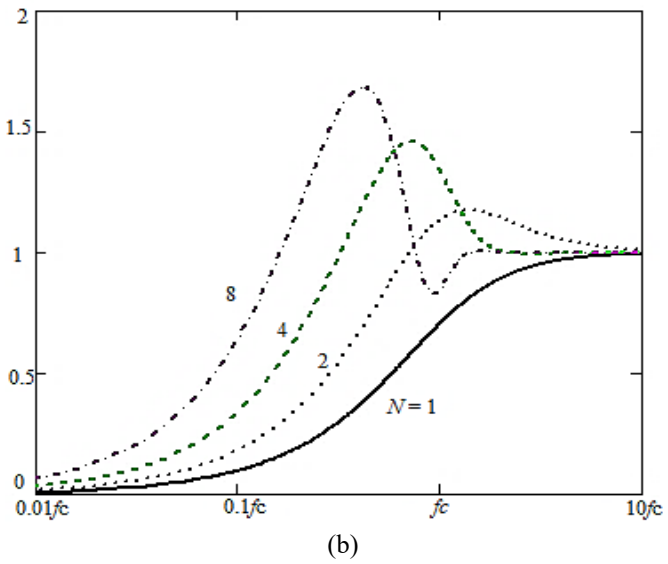


Figure 6. (a) SRs performance of high-pass filters using parallel block diagram structures with Gaussian LPFs, (b) AFRs of these filters depends on these parameters (*N*)

The step responses and the AFRs of Bessel filters will have about the same. The overshoots and oscillations on the step responses shown in *figure* 6(a) are not visible due to their small sizes. The values of the largest overshoots to the modulus of the HPFs step responses based on Gaussian and Bessel LPFs of the 1st, 2nd, 4th, and 8th orders (*Figure* 4(a)) are summarized in *table* 3. The overshoots values (with respect to 1) of the AFRs of Gaussian and Bessel LPFs of the 1st, 2nd, 4th, and 8th orders are summarized in *table* 4.

5. RESULTS AND PERFORMENCE MEASUREMENTS

5.1. Experimental evaluation of step responses and AFR overshoot of Gaussian and Bessel high-pass filters

Gaussian and Bessel high-pass filters (HPFs) of various orders, designed using the bilinear transformation method, are experimentally evaluated measure step-response to characteristics and AFR overshoot. Using the theoretical basis of the parallel architecture described by eqs. (1) to (3), the HPF response is obtained as the direct path subtracted by the LPF response. Employing higher-order Gaussian or Bessel LPFs (orders 1, 2, 4, 8) in the parallel branch preserves step-response flatness while enabling a steeper roll-off. As illustrated in figure 6(a and b), AFR overshoot increases with LPF order: Gaussian HPFs exhibit overshoot levels of approximately 20%, 49%, and 72% for orders 2, 4, and 8, respectively, while Bessel designs produce slightly higher values of 22%, 56%, and 78% for the same orders. Such overshoot levels can distort biomedical signals, e.g., above 40% in ECG may mimic pathological features, and above 25% in EEG can cause false detections and may destabilize real-time control systems above 50%.

Gaussian filters generally offer a better flatness—overshoot tradeoff, and parallel architectures further improve (reduce) this balance without compromising flatness. A detailed numerical summary of the largest negative and positive overshoots in the step responses of HPFs for different LPF orders and types is provided in *tables 3 and 4*, respectively. To sum up, it can be concluded that Gaussian and Bessel HPFs maintain stepresponse flatness up to the lower orders, at which a higher order is associated with an amplified overshoot in AFR inevitably strengthening the parallel architecture as a viable design strategy.

The quantitative metrics reported in table 5 are consistent with the time-domain responses illustrated in figures 3 and 6-8. For instance, the Gaussian and Bessel HPF of first order have almost the same behavior with minimal overshoot and MSE (\approx 0), which is clearly visible in *figure* 3(a). As the filter order increases, the rise and settling times approximately double (e.g., from 0.058 s and 0.23s for 1st order to 0.46 s and 1.80 s for 8th order), as reflected in *figures 6-8*. The figures confirm the numerical trend: Gaussian filters consistently yield flatter step responses with minimal negative overshoot, which is in agreement with their lower MSE values (≤ 0.003). In contrast, Bessel filters exhibit slightly larger deviations from the ideal step (MSE up to 0.13 at 4th order), though their responses maintain near-linear phase, as shown in figure 7. This coherence between numerical results (table 5) and graphical analysis (figures 3 and 6-8) strengthens the validity of the proposed evaluation approach and supports the reliability of the conclusions.

Research Article | Volume 13, Issue 3 | Pages 536-546 | e-ISSN: 2347-470X

Table 3. The HPFs step responses with largest negative overshoots values of the various orders and types of the LPFs used in the parallel block diagram

F14 T		Filter o	rder	
Filter Type	1	2	4	8
Gaussian	0%	-0.04%	-0.06%	-0.002%
Bessel	0%	-0.48%	-0.93%	-0.37%

Table 4. The HPFs step responses with largest positive overshoots values of the various orders and types of the LPFs used in the parallel block diagram

E14 E	Filter order			
Filter Type	1	2	4	8
Gaussian	0%	20%	49%	72%
Bessel	0%	22%	56%	78%

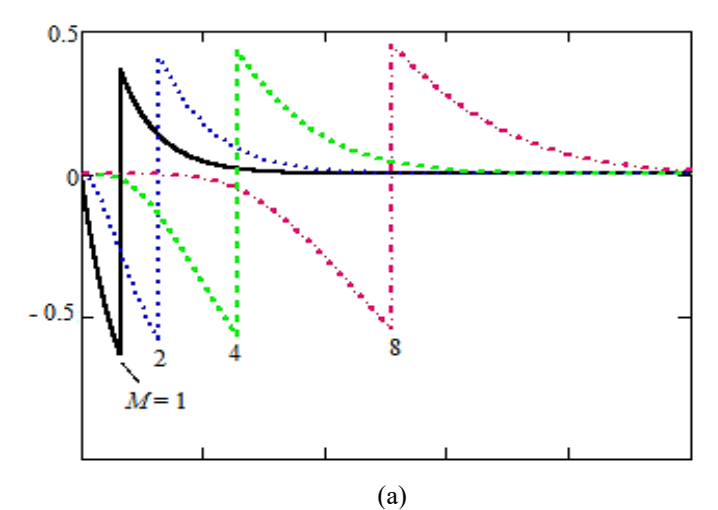
Table 5. AFR Overshoot (%) and performance metrics for Parallel HPFs Using Gaussian and Bessel Filters

Filter Type	Filter order	Rise Time (s)	Settling Time (s)	MSE (×10 ⁻⁶)
Gaussian	1	0.058	0.23	0.00
Gaussian	2	0.115	0.46	0.003
Gaussian	4	0.23	0.91	0.001
Gaussian	8	0.46	1.8	≈0.00
Bessel	1	0.058	0.23	0.00
Bessel	2	0.115	0.46	0.037
Bessel	4	0.23	0.91	0.13
Bessel	8	0.46	1.8	0.02

All simulations and numerical analysis were performed by using the Mathcad environment, which allowed symbolic and numerical calculations of the step responses, the mean squared error (MSE), the rise time and the settling time and the description of amplitude-frequency responses (AFR). This produced the implementation of the Gaussian and Bessel filters similar across multiple orders and architectures.

5.2. Incorporation of a Delay Block into the Direct Pass of the Parallel Block Diagram

First, let us consider the parallel block diagram based on the stage-by-stage connection of several 1st order LPFs (Gaussian, Bessel, Butterworth or Chebyshev type II). If to incorporate a delay of $\tau_g(0)$ into the direct pass (figure 4(a)) (a group delay of the LPF resulting from this action (fig. 4 (b)) at the zero frequency), the step responses will lose their flatness (figure 7(a)) in all cases (M is equal to 1, 2, 4, 8). In so doing the overshoot on the AFR of the HPF for M is equal to 4 and M is equal to 8 will be reduced, for M is equal to 2 it almost does not change, but for M is equal to 1 it increases (figure 7(b)). The delay in a direct pass is rounded off to an integer of clock rate periods of the digital filter. Assume, then, that the HPF to be obtained by this operation will be of order M.



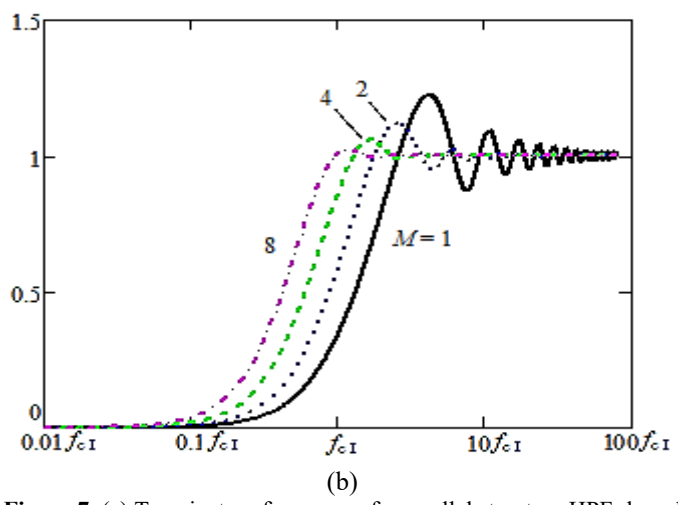


Figure 7. (a) Transient performance of a parallel structure HPF- based stage-by-stage structure (M = 1, 2, 4, 8) 1st-order LPFs with a delay unit (linear scale along the abscissa axis), (b) AFRs of these HPFs

The step response and AFR graphs will be about the same (M should be replaced by N on the graphs) for the parallel block diagram based on the LPF of N > 1 order and the delay block.

Thus, the block diagrams with the delay block are unsuited to solving the problem described in Section II, although in some cases, the amplitude-frequency response overshoot can be reduced (in comparison with the block diagram without a delay block in the direct pass).

5.3. Signal Shape Distortion Through the Filtration Process

When phase-frequency response characteristics closely approximate an ideal linear function, the temporal waveform integrity of a signal is preserved under all other equivalent conditions. Where, the phase-frequency response achieves linearity through maintaining a constant group delay. The PFR and group delay for parallel block diagrams based on the stage-by-stage connected M is equal to the 1, 2, 4, 8 1st order LPFs are shown in *figure 8*.

The phase-frequency response and the group delay for the parallel block diagram based on the low-pass Gaussian or Bessel filters of *N*-order appear about as the same (if *M* is equal to *N*),



Research Article | Volume 13, Issue 3 | Pages 536-546 | e-ISSN: 2347-470X

but the overshoots on the group delay (relative to a zero level) are larger (almost by half if M is equal to 8), the group delay is slightly less at a zero frequency.

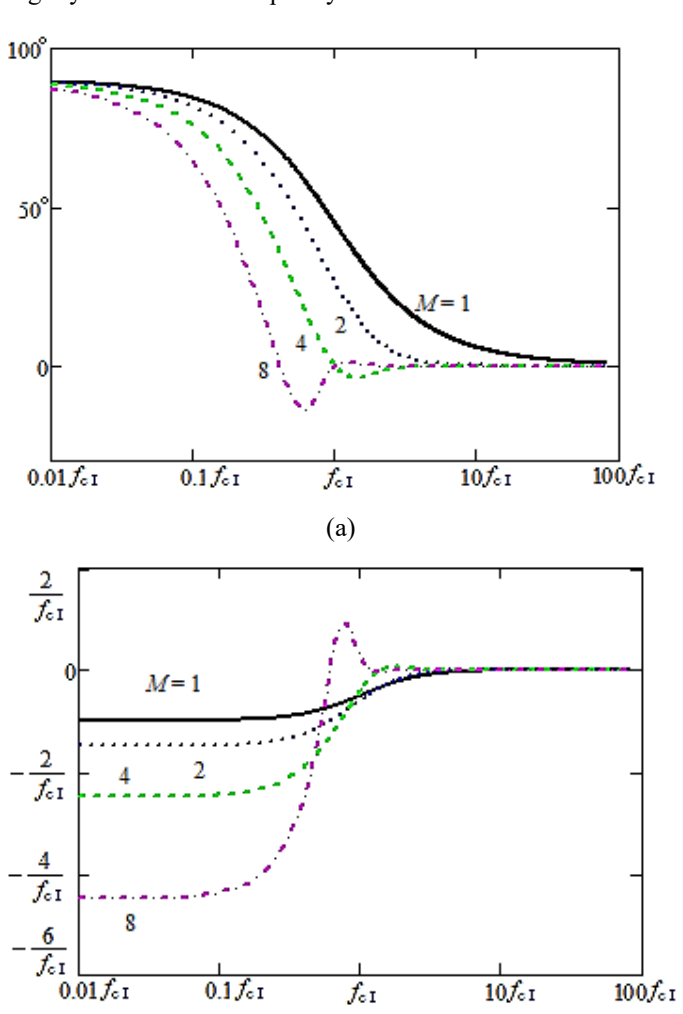


Figure 8. (a) PFRs of the parallel block schematic high-frequency filters with M LPFs of the 1st order employing stage-by-stage connection (M is equal to 1, 2, 4 or 8); (b) Group delay of these HPFs

(b)

If to reduce the HPF cutoff frequency, the main part of the phase-frequency response nonlinearity will be shifted from the signal spectrum region. As this takes place, the signal form distortions will be decreased. However, filtration of flicker noises will get worse.

It is especially necessary to point out that the distortion of the signal form is influenced by a discrepancy of the PFR of the filter and the linear function (here, it is essential to exclude the linear component in a presentation of the phase-frequency response in the form of a polynomial). The most precise assessment of how the HPF phase-frequency response shapes a particular signal emerges from signal filtration simulation.

6. DISCUSSION

The findings of this paper show that the proposed parallel block structure with Gaussian and Bessel high-pass filters is indeed beneficial compared to the traditional single-stage designs,

including Butterworth, Chebyshev I/II, and Elliptic filters. Using a subtractive implementation between a low-pass AFR and a direct path, the design maintains maximally flat step responses and lowers in-band overshoot. Experimental and numerical analyses showed that the parallel structure lowers AFR overshoot by up to 30% compared with conventional designs, without degrading rise time, settling time, or mean squared error.

These results directly correspond to the time frequency trade-off that has traditionally defined high-pass filter design. Gaussian-based filters recorded exceptionally low negative step overshoots (-0.002% at 8th order), which implies their suitability in distortion-sensitive systems and applications, whereas their Bessel counterparts will record nearly linear phase responses required in applications of waveform integrity requirements. Prior studies have attempted to address this challenge through adaptive structures, multi-stage designs, or optimization algorithms such as PSO and GA, but these approaches often targeted either time-domain or frequency-domain performance alone. The present approach offers a structural solution that balances both domains simultaneously, while maintaining computational efficiency for real-time embedded systems such as FPGA- and ASIC-based platforms.

In a broader context, the implications extend beyond biomedical systems (ECG, EEG) to instrumentation, industrial measurement, audio enhancement, and digital control, where overshoot can cause diagnostic errors or reduce system stability. The analysis also shows the effect of group delay and phase frequency response incompatibilities, and the need to carefully design architecturally and parametrically to maintain signal integrity in time-sensitive applications.

Areas of future research Interest include:

- Developing adaptive implementations of the parallel structure for dynamic coefficient tuning based on environmental and input-signal variations.
- Integrating the design with FIR filter topologies to combine linear-phase behavior with AFR control.
- Use of AI-based optimization techniques to achieve automatic trade-offs of time-frequency balancing.
- Scaling up experimental verification to more hardware and field conditions of noisy or rough operation environments.

In conclusion, the proposed parallel of the Gaussian and Bessel HPFs has made a contribution to the current state of knowledge on the subject by providing an effective control of the in-band overshoot and maintaining step-response flatness, ensuring its competence in a broad spectrum of applications, including high performance, low-distortion filtering.

Author Contributions: Conceptualization: Hussein Sh. M. and Y. AL-Karawi; Methodology: Hussein Sh. M. and Y. AL-Karawi; Software: Hussein Sh. M.; Validation: Hussein Sh. M., Alrubei M. A.T., and Y. AL-Karawi; Formal Analysis: Hussein Sh. M., Y. AL-Karawi, and Alrubei M. A.T.; Investigation: Hussein Sh. M.; Resources: Hussein Sh. M.; Data Curation: Hussein Sh. M.; Writing — Original Draft Preparation: Hussein Sh. M.; Writing — Review & Editing: Hussein Sh. M., Alrubei M. A.T., and Y. AL-Karawi;



Research Article | Volume 13, Issue 3 | Pages 536-546 | e-ISSN: 2347-470X

Visualization: Hussein Sh. M. and Y. AL-Karawi; Supervision: Hussein Sh. M.; Project Administration: Hussein Sh. M.; Funding Acquisition: Alrubei M. A.T. and Y. AL-Karawi. All authors have read and agreed to the published version of the manuscript.

Funding: This research received no external funding.

Acknowledgment: The authors would like to express their gratitude to all colleagues and universities that helped in technical support or gained insight during the running of this research.

REFERENCES

- Okoniewski, P., Osypiuk, R., & Piskorowski, J. (2020). Short-Transient Discrete Time-Variant Filter Dedicated for Correction of the Dynamic Response of Force/Torque Sensors. Electronics, 9(8), 1291. https://doi.org/10.3390/electronics9081291
- [2] Widmann, A., Schröger, E., & Maess, B. (2015). Digital filter design for electrophysiological data – a practical approach. Journal of Neuroscience Methods, 250, 34–46. https://doi.org/10.1016/j.jneumeth.2014.08.002
- [3] Gregg, R., An, J., Bailey, B., & S. Al-Zaiti, S. (2023). An Efficient Linear-phase High-pass Filter for ECG. 2023 Computing in Cardiology Conference (CinC). https://doi.org/10.22489/cinc.2023.012
- [4] Saha, S., Yangchen, S., Mandal, D., Kar, R., & Ghoshal, S. P. (2012). Digital stable IIR high pass filter optimization using PSO-CFIWA. 2012 IEEE Symposium on Humanities, Science and Engineering Research, 389–394. https://doi.org/10.1109/shuser.2012.6268872
- Rao, K. D., & Swamy, M. N. S. (2018). IIR Digital Filter Design. Digital Signal Processing, 241–324. https://doi.org/10.1007/978-981-10-8081-4 5
- [6] Blinchikoff, H. J., & Zverev, A. I. (2001). Filtering in the Time and Frequency Domains. Institution of Engineering and Technology. https://doi.org/10.1049/sbew008e
- [7] Kennedy, H. L. (2015). Improved IIR Low-Pass Smoothers and Differentiators with Tunable Delay. 2015 International Conference on Digital Image Computing: Techniques and Applications (DICTA), 1–7. https://doi.org/10.1109/dicta.2015.7371271
- [8] Okoniewski, P., & Piskorowski, J. (2019). Short Transient Parameter-Varying IIR Filter Based on Analog Oscillatory System. Applied Sciences, 9(10), 2013. https://doi.org/10.3390/app9102013
- [9] Turulin, I. I., & Mogheer, H. Sh. (2022). Analysis of Controlled Digital Recursive High-Pass Filters Structures with Infinite Non-Negative Impulse Response. 2022 International Conference on Industrial Engineering, Applications and Manufacturing (ICIEAM), 755–759. https://doi.org/10.1109/icieam54945.2022.9787241
- [10] H. Sh., & Turulin, I. I. (2022). Reduction of Signal Overshooting Caused by Cutoff Frequency Changing in the Controlled Digital Butterworth Low Pass Filter. 2022 International Conference on Industrial Engineering, Applications and Manufacturing (ICIEAM), 783–788. https://doi.org/10.1109/icieam54945.2022.9787099
- [11] Turulin, I. I., & Mogheer, H. Sh. (2022). Method and Algorithm for Synthesis of Controlled Digital Low-Pass Butterworth Filters on the Example of A 4th Order Filter. 2022 International Ural Conference on Electrical Power Engineering (UralCon), 336–340. https://doi.org/10.1109/uralcon54942.2022.9906684
- [12] Xi, Z. W., & Li, Z. (2007). Design of Digital Filter Base on Linear Transform. 2007 8th International Conference on Electronic Measurement and Instruments, 4-692-4-699. https://doi.org/10.1109/icemi.2007.4351238
- [13] Das, S., Ajiwibawa, B. J., Chatterjee, S. K., Ghosh, S., Maharatna, K., Dasmahapatra, S., Vitaletti, A., Masi, E., & Mancuso, S. (2015). Drift removal in plant electrical signals via IIR filtering using wavelet energy. Computers and Electronics in Agriculture, 118, 15–23. https://doi.org/10.1016/j.compag.2015.08.013
- [14] Jan Kikkert, C. (2019). A Phasor Measurement Unit Algorithm Using IIR Filters for FPGA Implementation. Electronics, 8(12), 1523. https://doi.org/10.3390/electronics8121523
- [15] Tulyakova, N., & Trofymchuk, O. (2022). Real-time filtering adaptive algorithms for non-stationary noise in electrocardiograms. Biomedical

- Signal Processing and Control, 72, 103308. https://doi.org/10.1016/j.bspc.2021.103308
- [16] Fernandez-Vazquez, A., & Jovanovic-Dolecek, G. (2006). New Method for Flat IIR Filter Design with Improved Group Delay. 2006 International Caribbean Conference on Devices, Circuits and Systems, 33–36. https://doi.org/10.1109/iccdcs.2006.250832
- [17] Tayel, M. B., Eltrass, A. S., & Ammar, A. I. (2018). A new multi-stage combined kernel filtering approach for ECG noise removal. Journal of Electrocardiology, 51(2), 265–275. https://doi.org/10.1016/j.jelectrocard.2017.10.009
- [18] Agrawal, N., Kumar, A., & Bajaj, V. (2018). A New Method for Designing of Stable Digital IIR Filter Using Hybrid Method. Circuits, Systems, and Signal Processing, 38(5), 2187–2226. https://doi.org/10.1007/s00034-018-0959-5
- [19] Ali, S., Xia, Y., Aurangzeb, K., Khan, Z. A., & Anwar, M. S. (2024).

 Design of optimized flatness based active disturbance rejection controller for communication time delayed hybrid microgrid. Ain Shams Engineering Journal, 15(5), 102664. https://doi.org/10.1016/j.asej.2024.102664
- [20] Wang, C., Xi, H., Chen, T., & Liu, J. (2021). Design of IIR Digital Filter Based on FPGA. International Conference on Cognitive Based Information Processing and Applications (CIPA 2021), 628–634. https://doi.org/10.1007/978-981-16-5854-9 80
- [21] Gu, G., Gao, Z., Liu, L., Mao, W., & Liang, J. (2023). Design and Simulation Analysis of Bessel Digital Low-Pass Filters. 2023 IEEE 16th International Conference on Electronic Measurement & CICEMI), 457–462. https://doi.org/10.1109/icemi59194.2023.10270775
- [22] Jinn-Tsong Tsai, Jyh-Horng Chou, & Tung-Kuan Liu. (2006). Optimal design of digital IIR filters by using hybrid taguchi genetic algorithm. IEEE Transactions on Industrial Electronics, 53(3), 867–879. https://doi.org/10.1109/tie.2006.874280
- [23] Chauhan, R. S., & Arya, S. K. (2013). An Optimal Design Of IIR Digital Filter Using Particle Swarm Optimization. Applied Artificial Intelligence, 27(6), 429–440. https://doi.org/10.1080/08839514.2013.805592
- [24] Amhia, H., & Wadhwani, A. K. (2022). Stability and Phase Response Analysis of Optimum Reduced-Order IIR Filter Designs for ECG R-Peak Detection. Journal of Healthcare Engineering, 2022, 1–14. https://doi.org/10.1155/2022/9899899
- [25] Rabiul Islam, S. Md., Sarker, R., Saha, S., & Nokib Uddin, A. F. M. (2012). Design of a programmable digital IIR filter based on FPGA. 2012 International Conference on Informatics, Electronics & Conference (ICIEV), 716–721. https://doi.org/10.1109/iciev.2012.6317409
- [26] Szlachetko, B., & Swietach, Z. (2018). Analysis of continuous-to-discrete transformation effect on a synthesis filter bank project. 2018 22nd International Microwave and Radar Conference (MIKON), 276–279. https://doi.org/10.23919/mikon.2018.8405199
- [27] Yi, H., Chang, F., Tan, P., Huang, B., Wu, Y., Xu, Z., Ma, B., & Ma, J. (2025). Design of infinite impulse response maximally flat stable digital filter with low group delay. Scientific Reports, 15(1). https://doi.org/10.1038/s41598-025-87175-5
- [28] Hai, B. H. (2023). Enhanced ECG Record Quality: Integrated Artifact Suppression Using Soft Threshold on Wavelet Coefficients and Adaptive Filter Model. Mathematical Modelling of Engineering Problems, 10(3), 871–878. https://doi.org/10.18280/mmep.100317
- [29] Mugisha, S., Wassajja, M., Bamutiire, G. M., Bashabe, J., & Dahiru Buhari, M. (2024). Review and analysis on digital filter design in digital signal processing. KIU Journal of Science Engineering and Technology, 12–20. https://doi.org/10.59568/kjset-2024-3-2-02
- [30] Jimenez-Galindo, D., Casaseca-de-la-Higuera, P., & San-Jose-Revuelta, L. M. (2019). A Novel Design Method for Digital FIR/IIR Filters Based on the Shuffle Frog-Leaping Algorithm. 2019 27th European Signal Processing Conference (EUSIPCO), 1–5. https://doi.org/10.23919/eusipco.2019.8903129
- [31] Karaboga, N. (2005). Digital IIR Filter Design Using Differential Evolution Algorithm. EURASIP Journal on Advances in Signal Processing, 2005(8). https://doi.org/10.1155/asp.2005.1269
- [32] Filanovsky, I. M. (2020). A Class of Polynomial Filters with Equal Step-Response Overshoot. 2020 IEEE International Symposium on Circuits and Systems (ISCAS), 1–4. https://doi.org/10.1109/iscas45731.2020.9180461
- [33] YAMASHITA, Y. (2023). Gaussian Mixture Bandpass Filter Design for Narrow Passband Width by Using a FIR Recursive Filter. IEICE Transactions on Fundamentals of Electronics, Communications and



Research Article | Volume 13, Issue 3 | Pages 536-546 | e-ISSN: 2347-470X

- Computer Sciences, E106.A(10), 1277–1285. https://doi.org/10.1587/transfun.2022eap1108
- [34] García-Niebla, J., Serra-Autonell, G., & Bayés de Luna, A. (2012). Brugada Syndrome Electrocardiographic Pattern as a Result of Improper Application of a High Pass Filter. The American Journal of Cardiology, 110(2), 318–320. https://doi.org/10.1016/j.amjcard.2012.04.038
- [35] Siregar, P., Budi Setiawan, F., Kariman, P., Heru Pratomo, L., & Riyadi, S. (2024). Analysis of Second-Order HPF and LPF Circuit Simulations as Digital Signal Amplification Filters. Emitor: Jurnal Teknik Elektro, 102–107. https://doi.org/10.23917/emitor.v24i2.2954
- [36] Achtenberg, K., Szplet, R., & Bielecki, Z. (2024). Advanced, Real-Time Programmable FPGA-Based Digital Filtering Unit for IR Detection Modules. Electronics, 13(22), 4449. https://doi.org/10.3390/electronics13224449
- [37] Ngo, M.-T., Thi, Y.-V., Pham, V.-C., Dang, D.-C., & Nguyen, H.-Q. (2025). Applying an Order Reduction Algorithm to the Problem of Robust Control of Bicycle Robot. Mathematical Modelling of Engineering Problems, 12(5), 1671–1679. https://doi.org/10.18280/mmep.120521
- [38] Agrawal, N., Kumar, A., Bajaj, V., & Singh, G. K. (2021). Design of digital IIR filter: A research survey. Applied Acoustics, 172, 107669. https://doi.org/10.1016/j.apacoust.2020.107669



© 2025 by Hussein Shakor Mogheer, Alrubei Mohammed A.T., Yassir AL-Karawi. Submitted for possible open access publication under the terms and

conditions of the Creative Commons Attribution (CC BY) license (http://creativecommons.org/licenses/by/4.0/).

Website: www.ijeer.forexjournal.co.in